Oxygen diffusion in the superconducting $YBa_2Cu_3O_{7-x}$

X. M. Xie, T. G. Chen, and Z. L. Wu
Shanghai Institute of Metallurgy, Academia Sinica, Shanghai, China 200 050
(Received 30 January 1989)

A low-frequency internal friction peak was observed at 200 °C for sintered $YBa_2Cu_3O_{7-x}$ bar specimens annealed at different temperatures between 400 and 650 °C. This peak is interpreted in terms of diffusional jumps of oxygen atoms in the basal planes between sublattice sites $O_A(\frac{1}{2}, 0, 0)$ and $O_B(0, \frac{1}{2}, 0)$. These two sites are not crystallographically equivalent in orthorhombic symmetry. Oxygen diffusivity for planar diffusion in the basal planes was derived on the basis of a one-dimensional random-walk process, which yields: $D=(\frac{1}{4})d^2C_B/(C_A+C_B)\nu_0\exp(-H_B/kT)=D_0\exp(-H_B/kT)$, where $H_B=H_A+\Delta E$. The parameters C_A, C_B, ν_0, and H_A are evaluated from internal friction data for the specimens of known oxygen deficiency x and ΔE, the potential energy difference between sites O_A and O_B, from Boltzmann's distribution law $C_A/C_B=\exp(-\Delta E/kT)$. The preexponential factor $D_0=3.5\times10^{-4}$ cm^2/sec and the activation energy of the 200 °C internal-friction peak $H_A=1.03$ eV are both temperature insensitive. By contrast, ΔE is temperature dependent; it is 0.23 eV at 400 °C and decreases as the temperature is raised, vanishing at 670 °C, the temperature of the orthorhombic-to-tetragonal transition temperature at which O_A and O_B sites become indistinguishable. Non-Arrhenius behavior exists between the oxygen diffusivity and the diffusion temperature in this type of diffusion mechanism.

INTRODUCTION

It is well known that the structure and electronic properties of $YBa_2Cu_3O_{7-x}$ depend only on the oxygen stoichiometry once the cation ratio Y:Ba:Cu=1:2:3 is fixed. The oxygen stoichiometry or rather, the oxygen number ($1-x$ per unit cell) decreases continuously as the annealing temperature is increased, with the structure and electronic properties changing accordingly.[1] Thus, in the range of $0.5>x>0$, the crystal is orthorhombic and superconducting, and T_c decreases continuously with increasing x until it drops to zero at $x\approx0.5$. For $x>0.5$, the compound is tetragonal and is no longer superconducting. The technology concerned with the preparation of superconducting $YBa_2Cu_3O_{7-x}$ involves two separate stages of atomic diffusion. (i) Pellets of the constituent oxide powders mixed in appropriate proportion are sintered at 920–950 °C, in which the $YBa_2Cu_3O_{7-x}$ compound is formed predominantly by voluminous cation diffusion. (ii) The sintered pellets are oxygenated in air or pure oxygen at low temperatures in order to optimize the superconducting properties by replenishment for oxygen up to a stoichiometry approaching 7. Low temperatures are favored in the second stage in which the cations are fixed in the lattice sites, leaving oxygen anions the only mobile species capable of long-range diffusion. However, the optimization of oxygen number to 1 (or $x=0$) cannot be realized, because the equilibrium temperature for a stoichiometric $YBa_2Cu_3O_7$ crystal under either oxygen or air ambient lies below 250 °C, at which oxygen mobility is practically suppressed to nil so that the oxygen replenishment can never be complete, leaving the real crystal always undercooled or in a metastable state. The highest oxygen content available to date is $YBa_2Cu_3O_{6.94}$.[2] It seems apparent that a knowledge of oxygen diffusion in this compound is urgently needed in order to facilitate the innovation of the manufacturing process so as to improve the quality of the material.

Data of oxygen diffusivity in superconducting $YBa_2Cu_3O_{7-x}$ oxide are much in controversy in the literature. It is well established that the rate of in-diffusion is much faster than the rate of out-diffusion.[3–6] The reason for this difference is not yet clearly understood. For oxygen in-diffusion in the sintered specimens within the temperature range of 200–400 °C, Glowacki *et al.*[6] obtained by differential scanning calorimetry an activation energy of $E=1.5-1.6$ eV and a preexponential factor $D_0=3-20$ cm^2/sec. Tu *et al.*[4,5] determined these parameters by *in situ* resistometry with $E=1.1\pm0.1$ eV at $x=0.38$ to $E=1.23$ eV at $x\approx0$, and $D_0=16$ cm^2/sec in the temperature range of 250–500 °C. The activation energy for oxygen diffusion $E=1.2$ eV is inconsistent with the results of Huang[7] and Ginley *et al.*[8]

Due to the porous and granular nature of the sintered material, internal friction (IF) is found to be especially suitable for investigating diffusion problems in such awkward specimens because in this method, the activated jumps of individual atoms akin to the elementary diffusion acts are measured irrespective of the macroscopic structure irregularities (e.g., porosity and grain boundaries, etc.) in the specimens. Detailed information concerned with the mechanism of the IF peak derivable from the classical theory of anelasticity[9] will provide important insight towards understanding of the diffusion characteristics.

The ideal, perfectly ordered structure of an $YBa_2Cu_3O_7$ unit cell with *Pmmm* symmetry is shown in Fig. 1(a). The structure features a one-dimensional (1D) Cu(1)-O(1)

chain weakly coupled through the highly asymmetric Cu(1)-O(4)-Cu(2) bonds to two two-dimensional (2D) CuO_2 planes. The atomic configuration in the basal plane (x-y plane at $z=0$) for this perfect crystal is shown in Fig. 1(b). Under equilibrium condition at absolute zero temperature, lattice sites O_A $(\frac{1}{2},0,0)$ are completely vacant and the sites O_B $(0,\frac{1}{2},0)$ are fully occupied by oxygen atoms. It will be shown later that site O_A is higher in potential energy than site O_B. A perfect crystal of $YBa_2Cu_3O_7$ possesses a maximum oxygen stoichiometry of 7 and the highest T_C of 93 K. Jorgensen *et al.*[10] were able to show that the superconducting properties of orthorhombic $YBa_2Cu_3O_{7-x}$ are uniquely determined by oxygen deficiency x in the basal plane in which both vacancy concentration and vacancy ordering are crucial. Due to the electronic coupling between the 1D Cu(1)-O(1) chain and the two 2D CuO_2 planes mediated by the bridging O(4) atoms, the change in electronic structure caused by oxygen deficiency in the chain affects the electronic properties of the two CuO_2 planes in such a way that is detrimental to superconductivity.

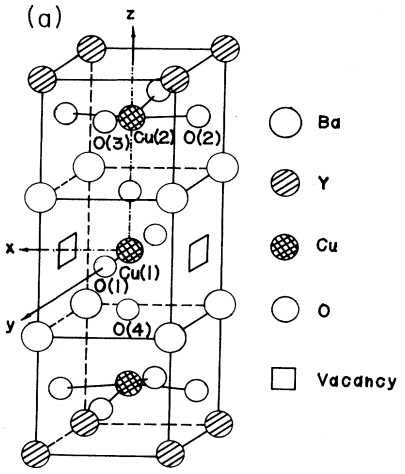

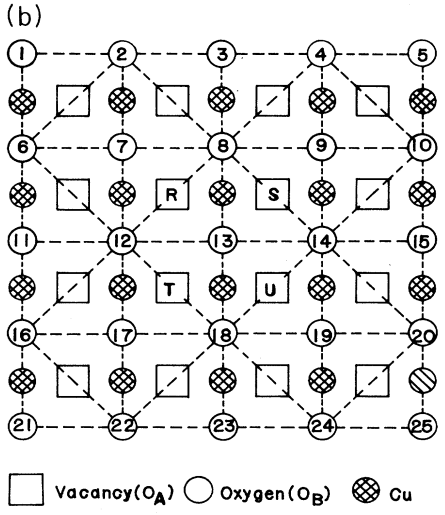

FIG. 1. (a) An unit cell of orthorhombic *Pmmm* $YBa_2Cu_3O_7$. (b) Atomic configuration in the basal plane of an $YBa_2Cu_3O_7$ crystal.

Under thermal equilibrium, the oxygen atoms in the basal plane are distributed among sites O_A and O_B according to Boltzmann's law: $C_A/C_B=\exp(-\Delta E/kT)$, where C_A and C_B are, respectively, the oxygen occupancies in sites O_A and O_B, and ΔE the potential energy difference between these two sites.

In the present work, a well developed IF peak was observed at 200 °C for the $YBa_2Cu_3O_{7-x}$ specimens with $x=0.12-0.46$. This peak was attributed to the diffusional jumps of the oxygen atoms in the basal plane. It was also found that the activation energies for the 200 °C peak and that for oxygen diffusion are different, owing to the potential energy difference between sublattice sites O_A and O_B. In the present paper, the mechanism of the 200 °C IF peak as well as its essential features are analyzed in detail and the oxygen diffusivities are derived from a one-dimensional random walk process in the basal plane. It is noteworthy to point out here that the IF described in this report is induced by the stress relaxation of individual atoms in the random walk process of diffusion and is entirely different from the low temperature IF reported by Duran *et al.*[11] originating from lattice deformation at the superconducting transition.

EXPERIMENTAL RESULTS

Specimen preparation and IF measurement

Powder with atomic ratio of Y:Ba:Cu=1:2:3 was prepared by co-deposition from nitrate solutions. The powder was calcined at 850 °C and then compressed into $50\times5\times2$ mm^3 bar specimens. Sintering was done at 930 °C for 18 h followed by furnace cooling. Six specimens were annealed in air at different temperatures (T_A) ranging from 400 to 650 °C for 10 h, then each was water quenched under the protection of a quartz sheath. The internal friction was measured at about 1 Hz in an automatic inverted torsional pendulum of the Kê type.

Figure 2 shows a typical internal friction curve mea-

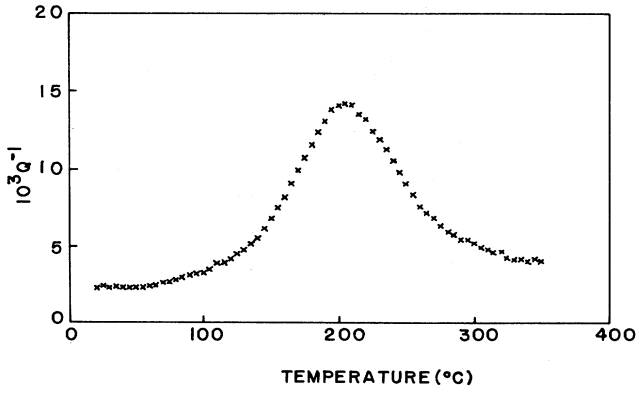

FIG. 2. Internal friction of a specimen annealed at and quenched from 400 °C.

TABLE I. Data for the 200 °C IF peak and for oxygen diffusion.

T_A(°C)	400	450	500	550	600	650
x[a]	0.12	0.19	0.26	0.32	0.39	0.46
T_p[b](°C)	197.7	199.0	199.5	202.4	205.9	219.7
$Q^{-1}_{max}\times10^3$	11.4	13.2	18.0	31.2	50.4	87.0
C_A	0.016	0.018	0.025	0.046	0.080[c]	0.183
C_B	0.805	0.762	0.695	0.604	0.500	0.337
H_A (eV)	1.02	1.02	1.02	1.03	1.04	1.08
H_B (eV)	1.25	1.26	1.25	1.22	1.18	1.13
ΔE (eV)	0.23	0.23	0.22	0.18	0.14	0.05
D_0 (10^{-4} cm^2/sec)	3.68	3.67	3.63	3.51	3.26	2.46
D(cm^2/sec)	1.69×10^{-13}	6.67×10^{-13}	2.86×10^{-12}	1.33×10^{-11}	5.30×10^{-11}	1.70×10^{-10}

[a] Reference 12, Fig. 6.
[b] Measured at 1 Hz.
[c] Reference 12, Fig. 7(b).

sured from a specimen annealed at $T_A=400$ °C prior to quenching. A peak of height 11.4×10^{-3} is observed at 200 °C. This peak, which is slightly broader than a single Debye relaxation peak, is caused by the superimposition of several subpeaks with slightly different activation energies. The height of the 200 °C peak increases rapidly with increasing temperature of annealing and at the same time the peak temperature is also slightly shifted towards the high-temperature side. Internal friction data measured from these six specimens are listed in Table I.

Activation energy for the 200 °C IF peak

Activation energy for this IF peak is the potential barrier a diffusing atom has to overcome for migration. The relaxation time for the diffusing atom is $\tau=\tau_0\exp(H_A/kT_p)$ where H_A is the height of the potential barrier and T_p the peak temperature. For the case of a Debye-type relaxation peak,[9] $\ln(\omega\tau)=0$. At the peak temperature, $\ln(\omega\tau_0)+H_A/kT_p=0$. Substituting $\omega=2\pi f$ into the above equation, we have $\ln(2\pi f\tau_0)+H_A/kT_p=0$, where f is the frequency of vibration of the specimen. Thus we can determine the magnitude of the potential barrier H_A by observing the frequency response of the peak temperature shift. $\ln f$ versus $1/T_p$ for the specimen annealed at 550 °C is plotted in Fig. 3.

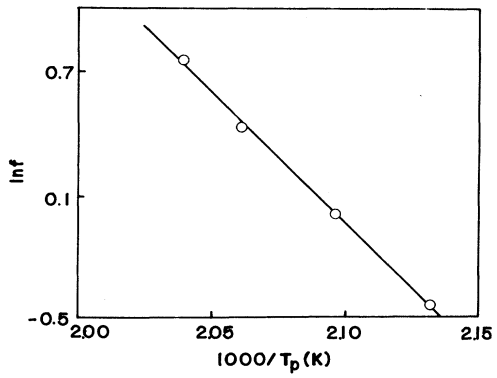

FIG. 3. Frequency response of the peak temperature ($T_A=550$ °C).

From the slope of the straight line shown in Fig. 3 and the above equation, we obtained $H_A=1.03$ eV and $\tau_0=2\times10^{-12}$ sec, or a frequency factor $\nu_0=5\times10^{11}$/sec. The activation energies for other specimens were obtained in the same way and the results are listed in Table I.

Potential energy differences between sites O_A and O_B

Because all the specimens have been subjected to a 10 h anneal at different annealing temperatures, we assume here that equilibrium between the oxygen content in the specimen and the ambient air has been established. In this case one expects the oxygen distribution between sites O_A and O_B to be Boltzmann-Maxwellian: $C_A/C_B=\exp(-\Delta E/kT_A)$. That is, site O_A is higher in potential energy than site O_B by ΔE. For each specimen annealed at temperature T_A, according to the theory of

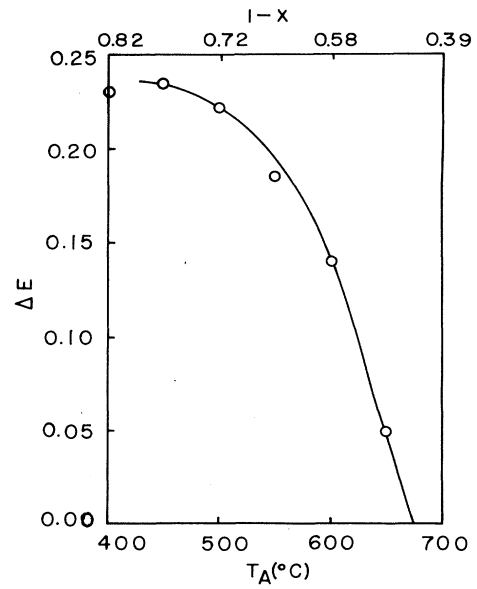

FIG. 4. Potential difference between sites O_A and O_B at different annealing temperatures.

anelastic relaxation to be discussed later, C_A and C_B can be calculated by Eqs. (3a) and (3b) (see Discussion) using the measured height of the 200 °C IF peak and the oxygen deficiency x listed in Table I. The values of ΔE so derived for other specimens are also listed in the same table. The relationship between ΔE and the annealing temperature T_A or oxygen number $1-x$ is shown in Fig. 4. As the annealing temperature is raised, C_A increases while C_B decreases (Table I); both decrease ΔE until at 670 °C $\Delta E=0$. This is the phase transition temperature of the compound; the latter transforms to the tetragonal phase and, at the same time, O_A and O_B become indistinguishable. The orthorhombic-to-tetragonal transition temperature 670 °C, found from the interception of the curve and the abscissa in Fig. 4, agrees well with the *in situ* neutron diffraction data by Jorgensen *et al.*[12]

DISCUSSION

The permissible and impermissible atomic jump

It is known that both atomic diffusion and a Snoek-type IF peak involve the migration of point defects. Neutron diffraction[10] has shown that within the temperature range of our experiment, point defects occur only in the basal planes. For the perfect $YBa_2Cu_3O_7$ crystal shown in Fig. 1(b), the O_A vacancies and O_B atoms are alternatively spaced along the diffusion paths $\langle 110\rangle$. One would like to know whether these regularly arrayed O_A sites could be treated as lattice vacancies allowing a direct atomic jump from site O_B to site O_A, e.g., a jump of atom O(7) to O_A vacancy (R) in Fig. 1(b). The 200 °C IF peak could then be explained by strain relaxation due to this elementary jump. The anelastic strain relaxation is caused by the lattice parameter change associated with an atomic jump which involves a local interchange of lattice parameters a and b ($a<b$). That such a mechanism for IF generation is possible has been demonstrated in a classical work of anelastic relaxation theory.[9] The defect symmetry of a vacancy-atom pair (or an O_A-O_B pair) is $\langle 110\rangle$ orthorhombic $Pmm2$, of the same order as the crystal symmetry of orthorhombic $Pmmm$. A diffusional jump of atom O(7) to site (R) would display an anelastic relaxation necessary for IF generation only if O_A and O_B were not crystallographically equivalent so that a chemical reaction could take place during the jump. The IF generated by this particular mechanism was called reaction-type by Nowick *et al.*[9] The nonequivalence for sites O_A and O_B has been demonstrated by the potential energy difference ΔE between these two sites. However, in the following we will show that a direct jump of an O_B atom into an O_A vacancy is not permitted, therefore the reaction-type internal friction described above does not exist in a perfect $YBa_2Cu_3O_7$ crystal.

If an O_B atom is permitted to jump into a nearest O_A vacancy, a perfect $YBa_2Cu_3O_7$ crystal ought to give the highest IF peak (say with a peak temperature at 200 °C). However, this conclusion is directly contradictory to our experimental results. Data listed in Table I show that the peak height is directly proportional to the concentration of oxygen vacancy, indicating the intrinsic defects in $YBa_2Cu_3O_{7-x}$ to be oxygen vacancies.

In Fig. 1(b), 16 $a\times b$ planar unit cells (in dotted squares) and 8 $(a^2+b^2)^{1/2}\times(a^2+b^2)^{1/2}$ supercells (in dashed rhombuses) are also drawn. An important characteristic of this perfect crystal is that the ratio [O]/[Cu]=1 in every supercell. This is the upper limit of oxygen content in the crystal giving the highest T_C of 93 K and a maximum oxygen stoichiometry of 7. However, a real crystal which contains dispersed frozen-in oxygen vacancies should embody many supercells having [O]/[Cu]<1. Atomic jumps only associate with these supercells. The occurrence of $(a^2+b^2)^{1/2}\times(a^2+b^2)^{1/2}\times c$ supercells resulting from traverse of the oxygen diffusion paths has been observed by Alorio-Franco *et al.*[13] at a low degree of oxygen deficiency with x as small as 0.1. This phenomenon and the occurrence of $2a\times b\times c$ superstructures at $x\approx 0.4$ strongly suggest that oxygen diffusion is operated by the vacancy mechanism.

In a perfect crystal in which [O]/[Cu]=1 in every supercell, a direct jump of an O_B atom into its nearest O_A site (vacant) is not permitted. For example, a jump of the O(7) atom into vacancy (R) will overcrowd supercell (8)-(12)-(18)-(14) to [O]/[Cu]=1.25, thus violating the [O]/[Cu]<1 rule for permissible atomic jumping. Only the supercell with [O]/[Cu]<1 is able to accept a jumping oxygen atom. On the contrary, in a real crystal with oxygen deficiency, say an O_B vacancy at position (13) in the supercell (8)-(12)-(18)-(14), the oxygen atom O(7) can jump to (R) without violating the [O]/[Cu]<1 rule. In order to make a jump of an oxygen atom O(7) permissible, the presence of an O_B vacancy at position (13) is required *a priori*. After the arrival of the diffusing atom at position (R), its potential energy is raised, rendering the atom in a metastable state. An additional jump can be easily driven by the applied alternating stress from position (R) to position (13) [or a back jump to position (7)] to restore its original state. As a consequence of the two successive jumps (7)$\rightarrow$(R)$\rightarrow$(13) ($O_B\rightarrow O_A\rightarrow O_B$), the diffusing atom at (7) and the O_B vacancy at (13) exchange their positions, i.e., one elementary diffusion act by the vacancy mechanism of length $d=(a^2+b^2)^{1/2}$ is accomplished. The only thing unique in the present case is the split of a diffusional jump into two substeps with the intermediate step in a metastable position. When an oxygen atom arrives at position (R), it always has two vacancies at its nearest-neighboring sites [position (7) and position (13) in Figs. 1(b) and 5] and it can jump forward or backward with equal probability. Therefore such a jump would be indistinguishable from a reversible reaction $A\rightleftharpoons B$, where products A and B are, respectively, oxygen atoms at sites O_A and O_B. There is no correlation between two successive jumps, indicating a random walk process occurring in the basal plane.

The diffusion path traversed by a diffusing atom in the elementary diffusion act is a straight line along [110] with a length of $(a^2+b^2)^{1/2}$. Likewise, an elementary diffusion act can also perform a zigzag path with a projected length $(\frac{1}{2})(a^2+b^2)^{1/2}$ along [110]. In case of high-vacancy concentration, it is possible to have two O_B vacancies existing in the corners of a single unit cell. For example, if the two atoms at positions (7) and (13) are

both missing, the oxygen atom at position (8) can jump first to position (R) then to position (7). This zigzag way of diffusion is important to the formation of the $2a\times b\times c$ superstructure to be discussed in a later section.

Up to now, we see that in a perfect crystal of stoichiometry $YBa_2Cu_3O_7$, the vacant O_A sites are not lattice vacancies in an ordinary sense, they are not permissible to the intercalation of oxygen atoms, except after being activated by the presence of one or two O_B vacancies sitting at the nearest-neighboring site of the O_A site in question. In other words, only these $(a^2+b^2)^{1/2}\times(a^2+b^2)^{1/2}\times c$ supercells with [O]/[Cu] <1 can admit a diffusing atom.

Noticeable evidence for the performance of the above atomic jump model in the diffusion process comes also from the observed difference between the in-diffusion and out-diffusion of oxygen in this material. According to the present model, the diffusion current is directly proportional to the density of the defective $(a^2+b^2)^{1/2}\times(a^2+b^2)^{1/2}\times c$ supercells (i.e., with [O]/[Cu] <1) because oxygen atoms are only admissible to these defective supercells.

For in-diffusion, oxygen stoichiometry in the materials is smaller than the equilibrium stoichiometry at the diffusion temperature. That means there are excess defective supercells in the original material. During the oxygenation anneal, the excess defective supercells are removed at first by oxygen replenishment in the outermost layer. The growth of this layer is controlled by oxygen diffusion through this layer. The density of defective supercells in the growth layer is maintained at the equilibrium value pertaining to the diffusion temperature. In the case of out-diffusion, the material is supersaturated with oxygen; in other words, it is depleted of defective supercells relative to the diffusion temperature. During the deoxygenation anneal, the outermost layer is first deprived of the oxygen atoms so as to increase the density of defective supercells to the equilibrium value corresponding to the diffusion temperature. However, the growth rate of the outside layer is controlled now by the rate of oxygen supply from the core to the interface between the growth layer and the core. That is, oxygen diffusion in the core is the limiting step for the out-diffusion process. Because the core is impoverished in defective supercells relative to the diffusion temperature, oxygen diffusion is suppressed to a rate slower than that in the growth layer. Therefore, the rate of oxygen desorption is remarkably slower than the rate of oxygen absorption.

Nature of the 200 °C IF peak

We assume in this section that (i) the 200 °C peak is a Debye-type relaxation peak induced by diffusional jumps of single particles with a peak height directly proportional to the concentration of the permissible diffusing particles, and (ii) that at the annealing temperature T_A, equilibrium solubility of oxygen has been built up so that the distribution of oxygen atoms in sites O_A and O_B is Boltzmann-Maxwellian. Based on these assumptions Nowick *et al.*[9] derived the observed peak height to be

$$Q_{\max}^{-1}=C_0C_AC_B/(C_A+C_B)\ , \tag{1}$$

where $C_0=v_0(\Delta\lambda)^2/(2J_ukT)$ and the relaxation time τ obeys

$$1/\tau=1/\tau_A+1/\tau_B=\nu_0\exp(-H_A/kT)+\nu_0\exp(-H_B/kT)\ . \tag{2}$$

C_0 is a constant independent of concentration, C_A and C_B are, respectively, the equilibrium oxygen occupancies at sites O_A and O_B, v_0 is the defect volume, $\Delta\lambda$ is the difference of strain tensor components along the b axis when an oxygen atom sits at an O_A site, and at an O_B site, J_u is the unrelaxed compliance of the crystal, and ν_0 the frequency of the diffusing atom endeavouring to pass the barriers H_A or H_B shown in Fig. 5. Setting $C_A+C_B=y$ and substituting it into Eq. (1), we have the solution

$$C_A=\frac{1}{2}\left[y-\left[y^2-\frac{4yQ_{\max}^{-1}}{C_0}\right]^{1/2}\right] \tag{3a}$$

and

$$C_B=y-C_A\ , \tag{3b}$$

where $y=1-x$ is the oxygen number in the basal plane of the compound $YBa_8Cu_3O_{7-x}$ with $0.5>x>0$. At $T_A=600$ °C, we find from Table I $C_A=0.08$ and $C_B=0.50$, and the measured $Q_{\max}^{-1}=5.04\times10^{-2}$. Substituting these values into Eq. (1), we obtain $C_0=0.73$. Oxygen stoichiometries x for different annealing temperatures and the measured peak heights corresponding to these temperatures are taken from Table I, and values of C_A and C_B calculated respectively from Eqs. (3a) and (3b). The values of C_A are now plotted against annealing temperature in Fig. 6. They fall consistently on the same curve with the neutron-diffraction data by Jorgensen

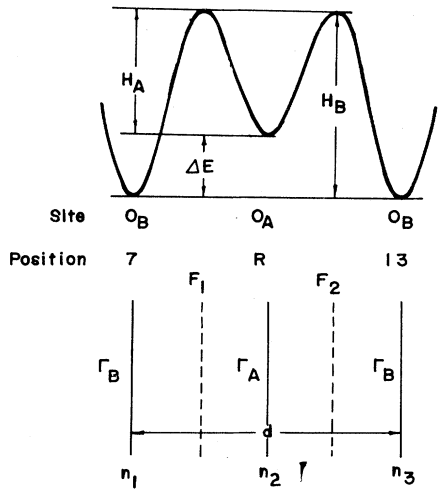

FIG. 5. Potential diagram for sites O_A and O_B. The intermediate state at O_A is metastable.

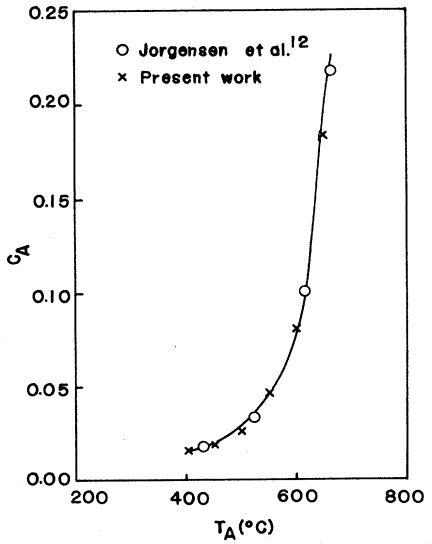

FIG. 6. Oxygen occupancy at O_A site (C_A) at different annealing temperatures (T_A).

et al.[12] Such a coincidence may largely be attributed to the application of the *in situ* data for y's and the so-derived constant C_0 in Eq. (3a). If we could obtain these experimental data from quenched specimens, the C_A versus T_A plot could be another curve of the same shape as that shown in Fig. 6. Jorgensen *et al.*[10] estimated the phase transition temperature for the quenched specimens to be 50–100 °C higher than that for the *in situ* specimens. That means the highest quenching temperature, 650 °C, used in our experiments is equivalent to 550 °C or so for the *in situ* specimens. At this temperature the ratio $C_A/C_B=0.046/0.604=0.076\ll 1$. In this case, Eq. (1) is reduced to

$$Q_{\max}^{-1}=C_0C_A \tag{3c}$$

indicating a linear relationship between peak height and oxygen occupancy in site O_A even at an annealing temperature as high as 650 °C. From Eq. (3c), one sees that the production of the 200 °C IF peak is principally dominated by the dilute concentration of oxygen atoms at O_A sites which execute a jump from site O_A to site O_B. From Fig. 5, we see that the activation energy from this jump is H_A.

Ordering of O_B vacancies

In deriving Eq. (1), it has been assumed that all the oxygen atoms in site O_A and O_B actively participate in diffusional jumps. The jump kinetics will be investigated in this section. Vacancy ordering gives rise a $2a\times b\times c$ superstructure as a result of the [O]/[Cu] < 1 restriction imposed on the permissible-impermissible atomic jumping model.

It is easily seen in Fig. 1(b) that an oxygen atom sitting at an O_A site is always accompanied by at least two O_B vacancies at its nearest ⟨110⟩ neighboring sites to which the diffusing atom can jump with equal probability. Therefore every oxygen atom in the O_A site is mobile. What we have to prove now is that the majority of the O_B atoms are also mobile or a concentration of mobile O_B atoms $C_{BM}\gg C_A$ so that Eq. (1) is reduced to Eq. (3c) and thus diffusion data can be obtained by internal friction measurement.

A vacancy occurring at position (13) will influence the jumping kinetics of all the O_B atoms within the square (7)-(9)-(19)-(17) consisting of four unit cells. By the application of the criterion [O]/[Cu] < 1 for a supercell capable of admitting an oxygen atom to distinguish a permissible and an impermissible atomic jump, we see that the corner atoms O(7), O(9), O(19), and O(17) are mobile while the four vortex-atoms O(8), O(14), O(18), and O(12) of the $(a^2+b^2)^{1/2}\times(a^2+b^2)^{1/2}\times c$ supercell are not. In this case, we have the vacancy concentration $x=\frac{1}{4}=0.25$, and the fraction of mobile atoms $=\frac{1}{3}=0.33$. From Table I it can be estimated that this value of x corresponds to that for $T_A=470$ °C. At this temperature, $C_A\approx 0.022$, $C_B\approx 0.73$ with $C_{BM}=0.24\gg C_A$ and therefore Eq. (3c) can still be applied. Now if we consider a pattern with vacancies at positions (7), (9), (13), (17), and (19), jumping kinetics of the oxygen atoms shown in Fig. 1(b) are influenced in this way: 8 atoms O(2), O(4), O(6), O(10), O(16), O(20), O(22), and O(24) are not permitted to jump; the others are all mobile. Here the vacancy concentration is $x=\frac{5}{16}=0.31$, and the fraction of mobile O_B atoms is $\frac{7}{11}=0.63$ and $C_{BM}\gg C_A$ again stands.

It is noteworthy to point out here that atom O(8) can jump in a zigzag way (8)→(*R*)→(7) without violating the [O]/[Cu] < 1 rule, so does atom O(18) traverse (18)→(*U*)→(19), leaving the 1D chain (3)-(23) three successive vacancies at (8), (13), and (18). Now if we extend this vacancy pattern one unit cell larger along each side, we have vacancies at positions (1), (3), (5), (11), (15), (21), (23), and (25) in Fig. 1(b) in addition to the original five. If such a pattern is embodied in a matrix of a perfectly ordered $YBa_2Cu_3O_7$ crystal, atoms influenced by this pattern form a 7×7 square array in which vacancy concentration $x=\frac{13}{36}=0.36$, and a fraction of mobile O_B atoms $=\frac{14}{23}=0.61$ and $C_{BM}\gg C_A$. In such a case, we have in the 1D chains (2)-(22) and (4)-(24) five successive vacancies, i.e., every other 1D chain in Fig. 1(b) is denuded of oxygen atoms. It has been pointed out by Alorio-Franco *et al.*[13] that oxygen deficiency in perovskite derived solids results in ordered rather than disordered oxygen vacancies. Therefore the occurrence of this highly ordered $2a\times b$ superstructure is energetically favorable in this type of crystal. In fact, the $2a\times b\times c$ superstructure has been observed by Chaillout *et al.*[14] in electron diffraction study using 620 °C annealed and then liquid nitrogen quenched specimens with $x=0.4$.

The pattern of the O_B vacancy array described previously simply illustrates that the performance of the permissible-impermissible atomic jumping model in vacancy ordering will lead to the formation of the $2a\times b\times c$ superstructure, but the kind of vacancy pattern bears no significance. The vacancy distribution within each grain cannot be homogeneous. The grain is divided into defect-rich and defect-lean regions. The size distribution

of these regions, vacancy concentration, as well as the pattern of vacancy array inside each region, change with temperature. However, these changes are accomplished by atomic jumps governed by the [O]/[Cu] < 1 rule outlined in the preceding section.

There are two steps in the T_C versus x curve[1,2] with two plateaus, respectively, at 90 K corresponding to $x=0-0.1$ and at 50 K corresponding to $x=0.3-0.4$. When x values are small ($x=0-0.1$), the vacancies are dispersed at random and their influence on the superconducting properties is small. In the range of $x=0.3-0.4$, long-range ordering brings forth the $2a\times b\times c$ superstructure; its influence on superconductivity is again small. Only in the stage of short range ordering, are the superconducting properties drastically impaired.

Under the items x, T_p, and H_A in Table I, one also sees that as the x value is increased, H_A and T_p increase accordingly, though in small amount. This increase in H_A may also be attributed to vacancy ordering. The latter is always associated with the interaction between diffusion particles. It is this inter-particle interaction which raises the potential barrier to a jumping atom, thus driving the IF peak toward the high-temperature side. However, from the data listed in Table I, the magnitude of the interaction is rather small.

One-dimensional random walk process in the basal plane

In this section we will derive the oxygen diffusivity in planar diffusion in the basal planes in terms of a one-dimensional random walk process along ⟨110⟩. Three planes each perpendicular to ⟨110⟩ at positions (7), (R), and (13) [Fig. 1(b)] are drawn in Fig. 5; oxygen concentration per unit area in these planes are, respectively, n_1, n_2, and n_3. Jumping frequencies of oxygen atoms at O_A and O_B are Γ_A and Γ_B. In the time interval $\delta t=1/\Gamma_A+1/\Gamma_B$, oxygen atoms at positions (7), (R), and (13) jump twice on average, and the diffusion currents passing through the two reference planes F_1 and F_2 are, respectively,

$$J_{F_1}\delta t=\tfrac{1}{2}n_1-\tfrac{1}{2}\tfrac{1}{2}n_1-\tfrac{1}{2}n_2+\tfrac{1}{2}\tfrac{1}{2}n_2-\tfrac{1}{2}\tfrac{1}{2}n_3 ,$$

$$J_{F_2}\delta t=\tfrac{1}{2}\tfrac{1}{2}n_1+\tfrac{1}{2}n_2-\tfrac{1}{2}\tfrac{1}{2}n_2-\tfrac{1}{2}n_3+\tfrac{1}{2}\tfrac{1}{2}n_3 .$$

After summing the above two equations and using the equation of continuity of flux $J_{F_1}=J_{F_2}=J$, we have

$$2J\delta t=\tfrac{1}{2}(n_1-n_3) ,$$

or

$$J=\tfrac{1}{4}(n_1-n_3)\frac{\Gamma_A\Gamma_B}{\Gamma_A+\Gamma_B} ,$$
$$n_1-n_3=(C_1-C_3)d=-\frac{\partial C}{\partial x}d^2 , \tag{4}$$

where $d=(a^2+b^2)^{1/2}$. Substituting the above equation into Eq. (4), we have

$$J=\left[-(\tfrac{1}{4})d^2\frac{\Gamma_A\Gamma_B}{(\Gamma_A+\Gamma_B)}\right]\frac{\partial C}{\partial X} ,$$

which is Fick's first law of diffusion $J=-D\partial C/\partial x$, with diffusivity

$$D=\tfrac{1}{4}d^2\frac{\Gamma_A\Gamma_B}{\Gamma_A+\Gamma_B} ,$$

where

$$\Gamma_A=\nu_0\exp(-H_A/kT) \quad \text{and} \quad \Gamma_B=\nu_0\exp(-H_B/kT) .$$

The number of oxygen atoms jumping from sites O_A to O_B equals that from sites O_B to O_A. Therefore we have $C_A\Gamma_A=C_B\Gamma_B$

$$D=\tfrac{1}{4}d^2\frac{C_B}{(C_A+C_B)}\nu_0\exp\left[-\frac{H_B}{kT}\right]=D_0\exp\left[-\frac{H_B}{kT}\right] , \tag{5}$$

where

$$D_0=\tfrac{1}{4}d^2\nu_0\frac{C_B}{(C_A+C_B)} \quad \text{and} \quad \nu_0=5\times10^{11}/\text{sec} .$$

By Eq. (5) the activation energy for oxygen diffusion is H_B and the potential diagram shown in Fig. 5 is therefore correct. Calculated D_0 values are listed in Table I. Values of D calculated from Eq. (5) are also listed in the same table. It should be pointed out here that the value of the preexponential factor D_0 reported in the literature[4-6] is 10^5 times larger than our results.

The preexponential factor D_0 and the activation energy for the IF peak H_A are practically independent of annealing temperature, while ΔE is temperature dependent, ranging from 0.23 eV at 400 °C to 0 at the phase transition temperature 670 °C (Fig. 4). This results in a decrease in activation energy for oxygen diffusion H_B with increasing temperature. Similar results have been observed by Tu *et al.*[4,5] who reported that the activation energy for oxygen in-diffusion in $YBa_2Cu_3O_{7-x}$ specimens decreases with increasing values of x.

However, no Arrhenius relationship exists between diffusivity D and the annealing temperature T_A because the ΔE part contained in H_B ($H_B=H_A+\Delta E$) is temperature dependent. This can clearly be seen in Fig. 7 where

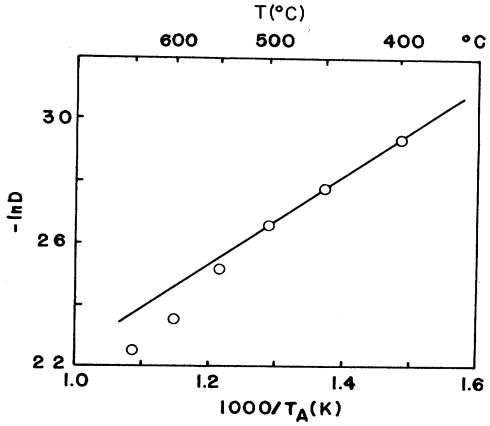

FIG 7. Diffusivity of oxygen in orthorhombic $YBa_2Cu_3O_{7-x}$ phase at different temperatures.

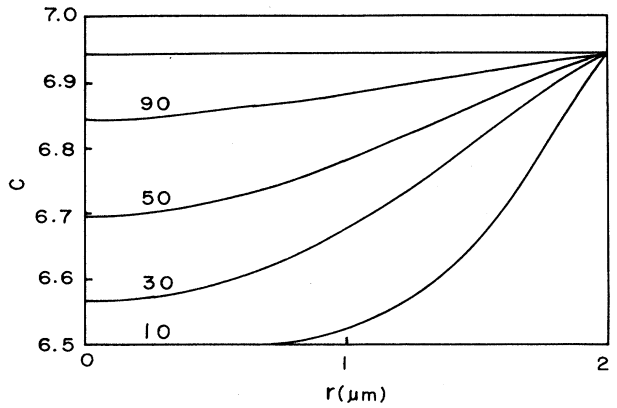

FIG. 8. Concentration profiles of oxygen for spherical diffusion at 350 °C for 10, 30, 50, and 90 h.

the $\ln D$ versus $1/T_A(K)$ plot is curved instead of being a straight line.

Oxygenation of sintered bulk specimens

For the sintered specimens with fine grains of random orientation, oxygen diffusivity can be derived from oxygen in-diffusion to a spherical particle of average grain size because the rate of oxygen convection in the gaseous phase and oxygen diffusion in the grain boundaries are much faster than the bulk diffusion in the grains. The grain size in our specimens is about 4 μm.[7] The concentration profile in spherical diffusion is[15]

$$\frac{C(r,t)-C_f}{C_f-C_i}=\frac{2r_0}{r}\sum_{n=1}^{\infty}\frac{(-1)^n}{n\pi}\sin\left[\frac{n\pi r}{r_0}\right]\times\exp\left[-\frac{Dn^2\pi^2 t}{r_0^2}\right], \quad (6)$$

where r_0 is the radius of the spherical particle, $r_0=2$ μm. $C(r,t)$ is the oxygen stoichiometry at the layer distant r radially from the center of the sphere at time t. If we anneal at 350 °C a specimen having $x=0.50$, then $D=2.82\times10^{-14}$ cm^2/sec is obtained by extrapolating the curve in Fig. 7 to 350 °C and $C_f=6.94$.[12] Here we take $C_i=6.50$ for convenience of illustration. Concentration profiles at $t=10$, 30, 50, and 90 h are respectively plotted in Fig. 8. According to the known T_C versus x relationship,[1,2] the 90 K phase has $x\leq0.12$. A 100-h air anneal at 350 °C is sufficient to transform the whole specimen to a 90 K superconducting phase.

ACKNOWLEDGMENTS

This work is supported by the National Science Foundation of China under Contract No. 5860300.

[1]A. J. Jacobson, J. M. Newsam, D. C. Johnston, D. P. Goshorn, J. L. Lewandowski, and M. S. Alvarez (unpublished).

[2]D. C. Johnston, A. G. Jacobson, J. M. Newsam, G. L. Lewandowski, D. P. Goshorn, D. Xie, and W. B. Yelon, in 194th Meeting of the American Chemical Society, New Orleans, 1987, edited by D. L. Nelson, M. S. Whittingham, and T. F. George (American Chemical Society, Washington, D.C., 1987), ACS Symp. Ser. No. 351, Chap. 14.

[3]K. N. Tu, S. I. Park, and C. C. Tsuei, Appl. Phys. Lett. **57**, 2158 (1987).

[4]K. N. Tu, C. C. Tsuei, S. I. Park, and A. Levi, Phys. Rev. B **38**, 772 (1988).

[5]K. N. Tu, N. C. Yeh, S. I. Park, and C. C. Tsuei, Phys. Rev. B **38**, 5118 (1988).

[6]B. A. Glowacki, R. J. Highmore, K. Peters, A. L. Greer, and J. E. Evett, Supercond. Sci. Technol. **1**, 7 (1988).

[7]J. Huang, Ph.D. thesis, Shanghai Institute of Metall. Academia Sinica, 1988 (unpublished).

[8]D. S. Ginley, P. J. Nigrey, E. L. Venturini, B. Borosin, and J. F. Kwak, J. Mater. Res. **2**, 732 (1987).

[9]A. S. Nowick and B. S. Berry, *Anelastic Relaxation in Crystalline Solids* (Academic, New York, 1972).

[10]J. D. Jorgensen, B. W. Veal, W. K. Kwok, G. W. Crabtree, A. Umezawa, L. J. Nowicki, and A. P. Paulikas, Phys. Rev. B **36**, 5731 (1987).

[11]C. Duran, P. Esquinazi, C. Fainstein, and M. Nuffez Regueiro, Solid State Commun. **65**, 957 (1988).

[12]J. D. Jorgensen, M. A. Beno, D. G. Hinks, L. Soderholm, K. J. Volin, R. L. Hitterman, J. D. Grace, I. K. Schuller, C. U. Segre, K. Zhang, and M. S. Kleefish, Phys. Rev. B **36**, 3608 (1987).

[13]M. A. Alorio-Franco, C. Chaillout, J. J. Capponi, J. Chenavas, Mater. Res. Bull. **22**, 1685 (1987).

[14]C. Chaillout, M. A. Alorio-Franco, J. J. Capponi, J. Chenavas, P. Strobel, and M. Marezio, Solid State Commun. **65**, 283 (1988).

[15]R. M. Barrer, *Diffusion in and Through Solids* (Cambridge University Press, Cambridge, 1951), Chap. 1.